Characterization and modeling of the viscoelasticity of pharmaceutical tablets

Léo Desbois, Pierre Tchoreloff, Vincent Mazel

Characterization and modeling of the viscoelasticity of pharmaceutical tablets

Léo Desbois[1], Pierre Tchoreloff[1], Vincent Mazel[1,*]

[1]Univ. Bordeaux, CNRS, Arts et Metiers Institute of Technology, Bordeaux INP, INRAE, I2M Bordeaux, F-33400 Talence, France

*corresponding author : Université de Bordeaux, I2M Bordeaux, 146 rue Léo Saignat, F-33000 Bordeaux, France ; tel :+33 5 57 57 92 60 ; E-mail address: vincent.mazel@u-bordeaux.fr

Abstract

Evolution of the compaction properties of powders with the compaction speed (strain rate sensitivity, SRS) is a common phenomenon during the manufacturing of pharmaceutical tablets. Nevertheless, several different phenomena can be responsible of the SRS like friction, viscoelasticity, viscoplasticity or air entrapment.In this work, an original experimental methodology was developed to characterize specifically the viscoelasticity of tablets using a compaction simulator. After various compressions, tablets were finally loaded elastically at different constant strain rates. This methodology made it possible to measure the apparent bulk and shear moduli as a function of the strain rate. The methodology was successfully applied to microcrystalline cellulose (MCC), Starch, Lactose monohydrate (GLac) and Anhydrous Calcium Phosphate (ACP). No significant evolution of the moduli was found for Lac and ACP as expected. On the contrary, for MCC and Starch, both shear and bulk moduli were found to increase along with the strain rate. The viscoelastic behavior was then successfully modeled using prony series. Assessment

of the model parameters was achieved by inverse identification using an analytical model and a finite element analysis.

keywords: viscoelasticity, compaction, speed, strain rate sensitivity, mechanical behavior, tablet

1. Introduction

The tablet is the most popular solid dosage form in the pharmaceutical industry. Nevertheless, the mechanical phenomena occurring during the manufacturing process are complex and still not fully understood. Even if the compaction process is used for more than a century, some manufacturing problems are still challenging today, like, for example, capping or sticking.

Scale-up is a critical aspect during the development of new tablets, because some problems may remain undetected during development. Historically, for the development of tablets, companies used eccentric presses whereas final production was generally performed on rotary presses. However, tablets produced on an eccentric machine might differ from those produced on rotary presses especially because the kinematic of this two kinds of presses is very different. To fill the gap, compaction simulators were created to be able, at the development scale, to mimic the kinematic behavior of the industrial rotary presses.

In fact, on industrial rotary presses, compaction speed can be very high and it is well known that this speed can have consequences on the final tablet quality attributes. This phenomena is often called Strain Rate Sensitivity (SRS)(Armstrong, 1989). Several aspects can explain the SRS. The first one is air entrapment. When the compaction speed increases, air can have difficulties to escape from the tablet and this can imply a modification of the apparent deformation behavior of the powder

(Casahoursat et al., 1988; Garr and Rubinstein, 1991). In addition, defects can appear inside or at the surface of the tablet (Long and Alderton, 1960; Mazel et al., 2015). Another factor is the kinematic friction between the powder/tablet and the die. It was shown that the kinematic friction coefficient increases with the sliding speed and that this speed dependency is an intrinsic property of the friction between a tablet and a die lubricated with magnesium stearate (Desbois et al., 2019).

Other aspects of the SRS are directly linked with the intrinsic mechanical properties of the compressed powder. Viscoplasticity means that the plastic deformation is time-dependent and viscoelasticity means that the elastic (recoverable) deformation is time-dependent (Alderborn and Nyström, 1996; Vincent, 2012). Both aspects have been studied (Çelik and Aulton, 1996; Katz and Buckner, 2013; Malamataris and Rees, 1993; Morehead, 1992; Radebaugh et al., 1989; Rees and Rue, 1978; Rippie and Danielson, 1981; Tye et al., 2005). Unfortunately, in the literature, the different aspects of the SRS are often mixed. To precisely define the SRS, it would be of interest to define a methodology that makes it possible to separate the different aspects.

This work is focused on viscoelasticity. In the literature, two main approaches were used to characterize viscoelasticity. The first one consists in characterizing the tablet after ejection (i.e. “out of die”). Several articles have presented methodologies with this approach using relaxation tests or dynamic mechanical analysis (Ascani et al., 2019; Çelik and Aulton, 1996; Hancock et al., 2001; Radebaugh et al., 1989). Nevertheless, these approaches have several drawbacks. First, only products that make it possible to obtain intact tablets after ejection can be used. Then, the forces used for the characterization are generally very low and far from the loads used during compaction. Finally, the characterization is often unidirectional, meaning that

only one elastic modulus is characterized in terms of viscoelasticity whereas a complete description would need the use of two different moduli.

The second method is to observe the viscoelasticity directly in the die, before tablet ejection. Several articles were published using a relaxation test at the compression top (Casahoursat et al., 1988; Rees and Tsardaka, 1993; Rehula et al., 2012). But at the compression top, both viscoelasticity and viscoplasticity are occurring. It is thus not a true viscoelastic characterization. Another approach is the use of the unloading part of the compaction cycle, where deformation is supposed to be elastic (Rippie and Danielson, 1981). Nevertheless, in the literature, it was also shown that plastic deformation takes place during most of the unloading step (Hiestand et al., 1977). Finally, other techniques were proposed like the use of ultrasounds (Saeedi Vahdat et al., 2013).

In this work, we propose an original experimental methodology to characterize specifically the viscoelasticity of a tablet directly in the die. This methodology makes it possible to separate viscoelasticity from the other kinds of time-dependent deformations.

Beyond the characterization of viscoelasticity, another objective of this study was to model the viscoelastic behavior with the objective of integrating this behavior in numerical simulations. Currently, Finite Element Method (FEM) is mainly used for the modelling of powder compaction. The models used (e.g. Drucker Prager Cap) are essentially time independent. In order to represent the viscoelastic behavior using FEM, a mathematical formulation of the viscoelastic behavior must be found. In this work, the time evolution of elastic moduli was represented using Prony series and

model parameters were found by inverse identification using an analytical approach and FEM simulations.

2. Material and method

2.1. Materials

2.1.1. Powders

Four pharmaceutical excipients were used: Lactose Monohydrate (GLac) (Excipress, ArmorPharma, Maen Roch, France), Anhydrous Calcium Phosphate (ACP) (DiCafos A60, Chemische Fabrik Budenheim, Budenheim, Germany), Microcrystalline Cellulose (MCC) (Vivapur200, JRS Pharma, Weissenborn, Germany) and Starch (Lycatab C, Roquette, Lestrem, France). Magnesium Stearate was used for external lubrication (Partek Mg Lub, Merck, Darmstadt, Germany).

2.1.2. Powder compaction

All compaction experiments were performed on a compaction simulator Styl'One Evolution (Medelpharm, Beynost, France). This machine is instrumented with load sensors (strain gauges) and displacement sensors (incremental sensors) on each punch. The die-wall pressure is measured with an instrumented die (strain gauge). For the experiments, round flat punches with a diameter of 11.28 mm were used.

An external system was used to lubricate the punches and the die. This system used a pulsed air blow cabinet to spray the Magnesium Stearate powder on the punches and die. Precise compaction conditions are explained below.

2.1.3. Numerical simulation

FEM was used for numerical modelling. All simulations were performed using the software Abaqus® (Abaqus® Standard 6.13, Dassault Systèmes, Vélizy-Villacoublay,

France). To represent the compaction process, the die and punches were modelled as analytical rigid surfaces and the tablet was defined as a continuous deformable solid. For symmetry reasons, axysymmetrical simulations were performed. A friction coefficient dependent of the speed was used to represent the friction between the tooling and the tablet during compression. Its value was taken from a previous publication (Desbois et al., 2019). Linear elastic and viscoelastic laws with Prony series were used.

2.2. Theoretical background: Linear viscoelasticity

In the case of linear elasticity, the relation between the strain of a solid (ε) and the applied stress (σ) can be represented by Hook's law:

$$\sigma = E\varepsilon \tag{1}$$

In the case of linear viscoelasticity, the previous equation can be replaced by an integral form (Marques and Creus, 2012):

$$\sigma(\mathrm{t}) = \int_0^t E(t-\tau)\frac{d\varepsilon(t)}{dt}d\tau \tag{2}$$

In this case, if Young's modulus depends on time, the stress-strain relationship is a function of the loading history (t=0 represents the beginning of the loading history).

Previous equations represent the 1D case. For 3D cases, it is possible to extend this approach using the deviatoric and volumetric parts of stresses and strains (Rippie and Danielson, 1981). This implies the use of the bulk (K) and shear (G) moduli. In these cases, the evolutions of the deviatoric (q) and the hydrostatic (p) stresses are given by the following relations (Marques and Creus, 2012):

$$q(t) = \int_0^t G(t-\tau)\frac{d\varepsilon_s(\tau)}{d\tau}d\tau \qquad (3)$$

$$p(t) = \int_0^t K(t-\tau)\frac{d\varepsilon_v(\tau)}{d\tau}d\tau \qquad (4)$$

with ε_s and ε_v the deviatoric and volumetric strains respectively.

To use equations (3) and (4), it is necessary to propose an analytical form of the time dependency of K and G. The most classical form is the Prony series. Prony series are derived from the generalized Maxwell model. They can be expressed as (Marques and Creus, 2012):

$$G(t) = G_\infty\left(1 + \sum_{i=1}^{n} g_i e^{-t/\tau_i}\right) \qquad (5)$$

$$K(t) = K_\infty\left(1 + \sum_{i=1}^{n} k_i e^{-t/\tau_i}\right) \qquad (6)$$

where G_∞ and K_∞ are the infinite shear and bulk moduli and g_i, k_i and τ_i are model parameters.

A complete characterization of the viscoelastic behavior of a solid using this model means the determination of all the constants included in the previous equations. This work presents a methodology for such a characterization.

2.3. Experimental protocol for the characterization of the viscoelasticity

To characterize viscoelasticity, it is important to design experiments where the tablet is deformed only elastically. This is for example not the case for relaxation experiments performed at the compaction top. For this purpose, a specific compaction cycle was defined and is presented in figure 1.

A first compression was performed to make the tablet. Furthermore, an extended dwell time was used to complete as much as possible the viscoplastic effects. This first compression defines the tablet that will be studied. In this work two first pressure levels were used: 100MPa and 200 MPa. Using these two different first pressures made it possible to obtained, for each product, tablets with two different porosity levels. These two values of pressure were chosen arbitrarily but are consistent with classical pressures used to obtain tablets. Thus, for each product, two sets of data will be presented: one for the tablets obtained under 100 MPa and one for the tablets obtained under 200 MPa.

After this first compression (either at 100MPa or at 200MPa), two more compressions with extended dwell times were performed at a pressure lower than the first one in order to complete as much as possible the plastic and viscoplastic deformations.

Finally, the viscoelastic properties were measured during the fourth compaction. The displacement during this compaction was set between 50 and 100 µm (depending on the product) which corresponds to a global strain between 1.75% and 3.5%. These values were chosen as a trade-off between a displacement value sufficiently high to ensure the precision of the measurements and overpass the initial non-linear elasticity (Brewin et al., 2007), and sufficiently low to remain in the linear viscoelastic domain. The compaction speed of this fourth step was varied in order to have loading times between 30 and 30000 ms with a nearly constant speed. Times were adjusted

as a function of the displacement to obtain, for each product, strain rates around 1, 0.1, 0.01 and 0.001s^{-1}. It must be noted that for ACP and GLac, it was not possible to obtained reliable results for the strain rate 1s^{-1}. So for these products only three strain rates will be presented. Times longer than 30000ms were not used because the normal compression time is often less than a few hundred milliseconds. The results presented here will thus focus on the viscoelasticity occurring during compression and not on very long term viscoelasticity (occurring during hours or days). With the compaction simulator used, it was also impossible to obtain a reliable signal for a compaction time under 30ms, especially because the speed was not constant during loading.

During the loading at different strain rate (or time), the viscoelastic behavior of a tablet can be approximated by an apparent linear elastic behavior, with apparent elastic constants that change from one loading time to another (Mattei and Ahluwalia, 2019). A previously published method (Mazel et al., 2012) was used to determine the apparent Young's modulus (E) and Poisson's Ratio (v). Finally, apparent K and G were calculated for the different loading times using the following equations (Landau and Lifshitz, 1959):

$$K = \frac{E}{3(1-2\nu)} \qquad (7)$$

$$G = \frac{E}{2(1+\nu)} \qquad (8)$$

For each condition, 5 tablets were produced.

3. Results and discussion

3.1. Experimental characterization of viscoelasticity

Before applying the methodology described above, it was important to verify that no viscoelastic effect was introduced by the press itself. The compaction system has indeed an elastic compliance, i.e. it deforms elastically during loading and unloading. It was thus important to verify that this elastic deformation was not time dependent. To measure the elastic deformation of the press, a steel gage was compressed between the two punches. The deformation of the gage, even if very small, was taken into account in the measure of the press deformation (Young's modulus of steel E=220 GPa). For this experiment, the gage was compressed between 0 and 90 MPa, which covers the range used in the fourth compression. This was done for compression times of 30, 300, 3000 and 30000 ms. This corresponds to the range of compression times used in our protocol for viscoelasticity determination. Results are presented in figure 2. The different runs are perfectly superimposed which means that no viscoelastic effect is introduced by the press itself. The elastic compliance of the press was taken into account in the measurement of the displacements.

The original in die method described above was then applied to four excipients to determine their viscoelastic behavior. The final porosities of the tablets obtained for each product and each pressure point are presented in table 1. No significant differences were found between tablets made with the same product and the same first pressure but with different loading time for the last compression. As a consequence, only one value of porosity for each first compression pressure is reported in table 1.

The apparent elastic moduli measured during the experiments are presented in table 2 and figures 3 and 4. For MCC and Starch, results in table 2 indicate that both K and G are dependent on the strain rate. More precisely, K and G increase when the strain rate increases, which is expected in the case of a viscoelastic product. To better

illustrate the variations, values of K and G normalized by the value obtained for the smallest strain rate (longest loading time) are presented in figures 3 and 4. For starch, at a strain rate of $0.1s^{-1}$, the increase was between 32% and 38% for G and between 21% and 24% for K. For MCC we obtained, for the same strain rate an increase of G and K between 14% and 20%, and 4% and 12% respectively. On the contrary, changes observed for ACP and GLac were always below 5% whatever the strain rate.

The excipients used in this study were chosen based on their mechanical behaviors as described in the literature. Starch is known to be a viscoelastic product and MCC present also some viscoelasticity (Malamataris and Rees, 1993; Van der Voort Maarschalk et al., 1997). On the contrary, ACP and GLac are not expected to show significant viscoelasticity. The results presented above are thus totally coherent with the existing literature: starch is the most viscoelastic of the four products and MCC also presents some viscoelasticity. On the contrary, the viscoelasticity of GLac and ACP is very low as expected. These results make it thus possible to validate the present methodology for the determination of the viscoelastic properties of pharmaceutical tablets. Based on these results, GLac and ACP show very limited viscoelasticity even if the strain rate range was three decades. Viscoelasticity can thus be neglected, on the time range studied in this work, in the mechanical behavior of these two products. The following parts of the article will thus focus on the results obtained on MCC and starch.

Besides showing that MCC and starch are indeed viscoelastic products, the methodology developed makes it possible to study both the volumetric and the deviatoric part of viscoelasticity. Generally, in the literature, the volumetric part of viscoelasticity is neglected compared to the deviatoric part. This was for example

done in the studies performed in the pharmaceutical field on the unloading part of the compaction profile (Rippie and Danielson, 1981). Such a hypothesis would mean that K should remain constant and that only G should vary with the strain rate. Results presented in figures 3 and 4 clearly show that the volumetric part of the viscoelasticity cannot be neglected in the case pharmaceutical tablets. Even if G shows greater variations than K, K is also varying with the strain rate.

As explained above, the purpose of using two different first compression pressures (100 MPa and 200 MPa) was to analyze the viscoelasticity with two different tablets for the same product. The results of the experiments reported in table 2 show differences between both compression pressures. As expected, for all the products and for each loading time, K and G increase when the first compression pressure increase, i.e, when the porosity decreases. This was expected according to the literature (Mazel et al., 2013; Roberts et al., 1994). In figures 3 and 4, a different evolution of the viscoelasticity of each product is found when the first pressure varies. When the first compression pressure increases (i.e. reduced porosity, see table 1), normalized G and K increase for Starch, however, for MCC the normalized moduli decrease. These results imply two different behaviors. For Starch the viscoelasticity increases and for MCC the viscoelasticity decreases when the porosity decreases. These results are very preliminary, and a complete understanding of this phenomena would require further work that overpasses the objectives of this study.

Finally, the proposed characterization method made it possible to characterize the viscoelasticity of the different products qualitatively and quantitatively. For each product, we obtained a couple of K and G associated with a loading time. The following objective of this work was to find a model that represents correctly this viscoelastic behavior and that could be introduced in FEM simulation.

3.2. Modeling of the viscoelastic behavior

As explained above, to be able to use equations (3) and (4) to represent the viscoelastic behavior of the powders, it is necessary to choose an analytical expression of K and G. As often done, Prony series were chosen in this study for this purpose. The objective of this part is to determine the coefficients of the Prony series for G and K that make it possible to represent the viscoelastic behavior found in the previous experiments for Starch and MCC. The first step was to find approximate coefficients of the Prony series with an analytic approach. In a second step, using FEM simulation, friction between the die and the tablet was taken into account.

3.2.1. Analytical development of the Prony series

In our experiments, the loading speed is constant, which implies that the strain rate is also approximately constant:

$$\frac{d\varepsilon(\tau)}{d\tau} = \frac{\varepsilon}{t} = A \qquad (9)$$

with A the strain rate (s^{-1}) .

In this case, the integrals from equations 3 and 4 can be easily calculated. The results for the evolution of q and p as a function of time can be found in the following equations:

$$q(t) = AG_\infty \left[t + \sum_{i=1}^{n} g_i \, e^{-t/\tau_i} \times \tau_i \left(e^{t/\tau_i} - 1 \right) \right] \qquad (10)$$

$$p(t) = AK_\infty \left[t + \sum_{i=1}^{n} k_i \, e^{-t/\tau_i} \times \tau_i \left(e^{t/\tau_i} - 1 \right) \right] \qquad (11)$$

Using equations (10) and (11), it is possible to calculate the apparent K and G for the different loading times. The apparent moduli found are function of the parameters of the prony series. The aim was then to find the parameters of the prony series that make it possible to obtain analytically apparent moduli close to those found experimentally.

The first step was to decide how many terms to use in the prony series. It is common to consider one characteristic time (τ_i) per decade. Considering the analytical protocol developed, we chose to use three characteristic times: 30 ms, 300ms and 3000ms. We thus used Prony series with three terms.

The experiments at 30000 ms were considered as quasi-static and were used as a first approximation for K_∞ and G_∞. Finally, to determine the different g_i and k_i , a reverse identification with the experiments was performed. g_i and k_i values were adjusted manually until the apparent moduli calculated matched the experimental values.

Comparison between the experimental and calculated values at the end of the adjustment process can be found in table 3. As it can be seen, the Prony series make it possible to represent the viscoelastic evolution obtained experimentally with a great precision (errors are always lower than 1%).This shows that the analytical approach proposed gives very good results. Nevertheless, it contains simplifications compared to the performed experiments. Indeed, it considers that the whole tablet is submitted to homogeneous stresses, which is not strictly correct because of the friction between the tablet and the die. Moreover, friction between the tablet and the die was found previously to depend on the speed of compaction (Desbois et al., 2019). In order to take into account these effects, the finite element method was finally used.

3.2.2. Finite element method integration

As mentioned previously, all the simulations were performed using the software Abaqus®. Viscoelasticity based on prony series is already implemented in the code. Nevertheless, in Abaqus®, Prony series formulation is slightly different from the expression presented above. In equation 5 and 6, g_i and k_i correspond to moduli normalized with respect to the infinite moduli (G_∞,K_∞). In Abaqus, the parameters correspond to moduli normalized with respect to the initial moduli. The parameters calculated above had thus to be transformed in order to be implanted in the code. Nevertheless, for clarity reasons, in the following text, we will still express the parameters of the Prony series based on infinite moduli as formulated in equation 5 and 6.

The simulations carried out represent compressions with the experimental loading times (30ms, 300ms, 3000ms). The simulation generates the evolution of the axial and radial forces and the thickness of the tablet. These values were used to calculate the stresses and strains on the tablet during the loading and thus to determine the apparent elastic moduli as explained above.

The simulations were first performed with the parameters determined analytically, then parameters were varied to find apparent moduli as close as possible to the experimental values. The calculations were applied to the two viscoelastic products studied before, MCC and starch.

The only difference between the analytical approach and the FEM approach is the introduction of friction. The results obtained in the simulation showed that friction only promotes a slight increase of all the apparent moduli of a nearly constant value. As a consequence, to improve the correspondence between simulated and experimental

values it was only found necessary to lower slightly (around 0.5%) the infinite moduli without changing the g_i and k_i parameters. The values obtained were very similar to those presented in table 3 with an error between the experimental and the numerical values always lower than 1%. This means that Prony series are well suited to represent the viscoelastic behavior of pharmaceutical tablet during FEM modelling.

Table 4 shows the coefficients of the Prony series used in the simulations for MCC and Starch. The g_i and k_i show the same trend as those found in Figure 3 and Figure 4. For example, the g_i are higher than the k_i which means that the deviatoric behavior is more important than the volumetric behavior. Nevertheless, the parameters make it possible to go a little bit further in the characterization of the viscoelastic behavior because they give access to the importance of the different characteristic times. It is interesting to note that viscoelasticity is present at both long and short characteristic times. Viscoelasticity at long characteristics times was expected. It is indeed well-known that tablets of starch or MCC keep expending after ejection and that this expansion continues during several hours. The term at 3000 ms could correspond to an expansion just after unloading. Of course, it is possible that longer times might also be present but they overpass the objectives of this study which is more focused on the characteristic times occurring during compression.

The results presented in table 4 also show that viscoelasticity is not limited to long times. The term at 30ms is important in all the cases. Especially, in the deviatoric part, this term is always the largest. The short time terms are those which are the most important during compaction (the compaction cycle is generally much less than 1s). This means that viscoelasticity indeed plays a role during compaction. Thus, including it for example in numerical modelling is mandatory to correctly represent the compaction behavior of certain kind of products.

4. Conclusion

Strain rate sensitivity during tablet manufacturing is a complex phenomenon. It is composed of different phenomena like air entrapment, kinematic friction, viscoplasticity or viscoelasticity. The methodology developed in this work made it possible to isolate the viscoelasticity of the material with a special compression cycle using different strain rates. Four different pharmaceutical excipients were studied with success and it was found, as expected, that GLac and ACP have very limited viscoelasticity, contrary to MCC and starch. Moreover, Starch was found more viscoelastic than MCC.

Prony series were used to represent analytically the viscoelastic behavior. Prony series terms were first identified using an analytical approach. Then a FEM numerical approach was used to refine the results by taking friction into account. It was found that Prony series made it possible to correctly represent the viscoelastic behavior of pharmaceutical tablets. Moreover, the Prony series parameters obtained made it possible to quantify the viscoelastic behavior.

In addition to a new methodology to quantify viscoelasticity, the present study highlights two important results. First, in the case of pharmaceutical tablets, viscoelasticity is not limited to deviatoric terms. The volumetric part, even if less important, cannot be neglected, contrary to what was supposed in the pharmaceutical literature. The other point is that viscoelasticity is present at short and long times. The short time terms indicate that viscoelasticity might play a role during compaction and not only during post compaction relaxation. It must be noted that shorter times effects might also be present but that it was not possible to characterize them with the present methodology.

As shown in this article, the apparent elastic moduli of a pharmaceutical tablet might be influenced by the strain rate. This is important to consider when comparing results of elastic moduli found in different studies as tableting conditions might differ greatly from one study to the other.

Finally, Prony series could be used in numerical simulation to represent the viscoelastic behavior of a powder during compression. Nevertheless, some code limitation may arise. For example, in the current version of Abaqus® (6.13), it is not possible to use simultaneously viscoelasticity and plasticity. The use of this model might thus require the development of user defined mechanical behavior in FEM codes.

Acknowledgement

The authors acknowledge the support of the French Agence Nationale de la Recherche (ANR), under grant ANR-17-CE08-0015 (project CliCoPha).

Legend to figures

Figure 1: Typical evolution of the compaction pressure vs time for the proposed protocol: a) Example of evolution during the whole compaction cycle; b) Examples of 4^{th} compactions at different strain rates.

Figure 2: Total press deformation as a function of the axial pressure for different compression times.

Figure 3: Normalized shear modulus as a function of the strain rate.

Figure 4: Normalized bulk modulus as a function of the strain rate.

References

Alderborn, G., Nyström, C., 1996. Pharmaceutical powder compaction technology. Marcel Dekker, New York.
Armstrong, N.A., 1989. Time-dependent factors involved in powder compression and tablet manufacture. International Journal of Pharmaceutics 49, 1–13.
Ascani, S., Berardi, A., Bisharat, L., Bonacucina, G., Cespi, M., Palmieri, G.F., 2019. The influence of core tablets rheology on the mechanical properties of press-coated tablets. European Journal of Pharmaceutical Sciences 135, 68–76. https://doi.org/10.1016/j.ejps.2019.05.011
Brewin, P.R., Coube, O., Doremus, P., Tweed, J.H., 2007. Modelling of Powder Die Compaction. Springer Science & Business Media.
Casahoursat, L., Lemagnen, G., Larrouture, D., 1988. The Use of Stress Relaxation Trials to Characterize Tablet Capping. Drug Development and Industrial Pharmacy 14, 2179–2199.
Çelik, M., Aulton, M.E., 1996. The Viscoelastic Deformation of Some Tableting Materials as Assessed by Indentation Rheology. Drug Development and Industrial Pharmacy 22, 67–75.
Desbois, L., Tchoreloff, P., Mazel, V., 2019. Influence of the Punch Speed on the Die Wall/Powder Kinematic Friction During Tableting. JPharmSci 108, 3359–3365.
Garr, J.S.M., Rubinstein, M.H., 1991. An investigation into the capping of paracetamol at increasing speeds of compression. International Journal of Pharmaceutics 72, 117–122.
Hancock, B.C., Dalton, C.R., Clas, S.-D., 2001. Micro-scale measurement of the mechanical properties of compressed pharmaceutical powders. 2: The dynamic moduli of microcrystalline cellulose. International Journal of Pharmaceutics 228, 139–145.
Hiestand, E.N., Wells, J.E., Peot, C.B., Ochs, J.F., 1977. Physical processes of tableting. J. Pharm. Sci. 66, 510–519.
Katz, J.M., Buckner, I.S., 2013. Characterization of strain rate sensitivity in pharmaceutical materials using indentation creep analysis. International Journal of Pharmaceutics, Manufacturing Performance of Solid Dosage Forms 442, 13–19.
Landau, L.D., Lifshitz, E.M., 1959. Theory of Elasticity, Course of theoritical physics. Pergamon Press, London.
Long, W.M., Alderton, J.R., 1960. The displacement of gas from powders during compaction. Powder Metallurgy 3, 52–72.
Malamataris, S., Rees, J.E., 1993. Viscoelastic properties of some pharmaceutical powders compared using creep compliance, extended Heckel analysis and tablet strength measurements. International Journal of Pharmaceutics 92, 123–135.
Marques, S.P.C., Creus, G.J., 2012. Computational Viscoelasticity. Springer, Berlin Heidelberg.
Mattei, G., Ahluwalia, A., 2019. A new analytical method for estimating lumped parameter constants of linear viscoelastic models from strain rate tests. Mech Time-Depend Mater 23, 327–335.
Mazel, V., Busignies, V., Diarra, H., Tchoreloff, P., 2015. Lamination of pharmaceutical tablets due to air entrapment: Direct visualization and influence of the compact thickness. International Journal of Pharmaceutics 478, 702–704.
Mazel, V., Busignies, V., Diarra, H., Tchoreloff, P., 2013. On the Links Between Elastic Constants and Effective Elastic Behavior of Pharmaceutical Compacts:

457 Importance of Poisson's Ratio and Use of Bulk Modulus. Journal of
458 Pharmaceutical Sciences 102, 4009–4014.
459 Mazel, V., Busignies, V., Diarra, H., Tchoreloff, P., 2012. Measurements of elastic
460 moduli of pharmaceutical compacts: A new methodology using double
461 compaction on a compaction simulator. J. Pharm. Sc.
462 Morehead, W.T., 1992. Viscoelastic Behavior of Pharmaceutical Materials During
463 Compaction. Drug Development and Industrial Pharmacy 18, 659–675.
464 Radebaugh, G.W., Babu, S.R., Bondi, J.N., 1989. Characterization of the viscoelastic
465 properties of compacted pharmaceutical powders by a novel nondestructive
466 technique. International Journal of Pharmaceutics 57, 95–105.
467 Rees, J.E., Rue, P.J., 1978. Time-Dependent Deformation of Some Direct
468 Compression Excipients. Journal of Pharmacy and Pharmacology 30, 601–
469 607.
470 Rees, J.E., Tsardaka, K.D., 1993. Compaction stress relaxation interpreted using a
471 hyperbolic relation. International Journal of Pharmaceutics 92, 137–141.
472 Rehula, M., Adamek, R., Spacek, V., 2012. Stress relaxation study of fillers for
473 directly compressed tablets. Powder Technology 217, 510–515.
474 https://doi.org/10.1016/j.powtec.2011.11.011
475 Rippie, E.G., Danielson, D.W., 1981. Viscoelastic stress/strain behavior of
476 pharmaceutical tablets: Analysis during unloading and postcompression
477 periods. J. Pharm. Sci. 70, 476–482.
478 Roberts, R.J., Rowe, R.C., York, P., 1994. The Poisson Ratio of Microcrystalline
479 Cellulose. International Journal of Pharmaceutics 105, 177–180.
480 Saeedi Vahdat, A., Krishna Prasad Vallabh, C., Hancock, B.C., Cetinkaya, C., 2013.
481 Ultrasonic approach for viscoelastic and microstructure characterization of
482 granular pharmaceutical tablets. International Journal of Pharmaceutics, A
483 Position Paper and Commentaries on More effective advanced drug delivery
484 systems 454, 333–343. https://doi.org/10.1016/j.ijpharm.2013.06.045
485 Tye, C.K., Sun, C. (Calvin), Amidon, G.E., 2005. Evaluation of the effects of tableting
486 speed on the relationships between compaction pressure, tablet tensile
487 strength, and tablet solid fraction. Journal of Pharmaceutical Sciences 94,
488 465–472. https://doi.org/10.1002/jps.20262
489 Van der Voort Maarschalk, K., Zuurman, K., Vromans, H., Bolhuis, G.K., Lerk, C.F.,
490 1997. Stress relaxation of compacts produced from viscoelastic materials.
491 International Journal of Pharmaceutics 151, 27–34.
492 Vincent, J., 2012. Structural Biomaterials, Third edition. ed. Princeton University
493 Press, Princeton.
494

495

496

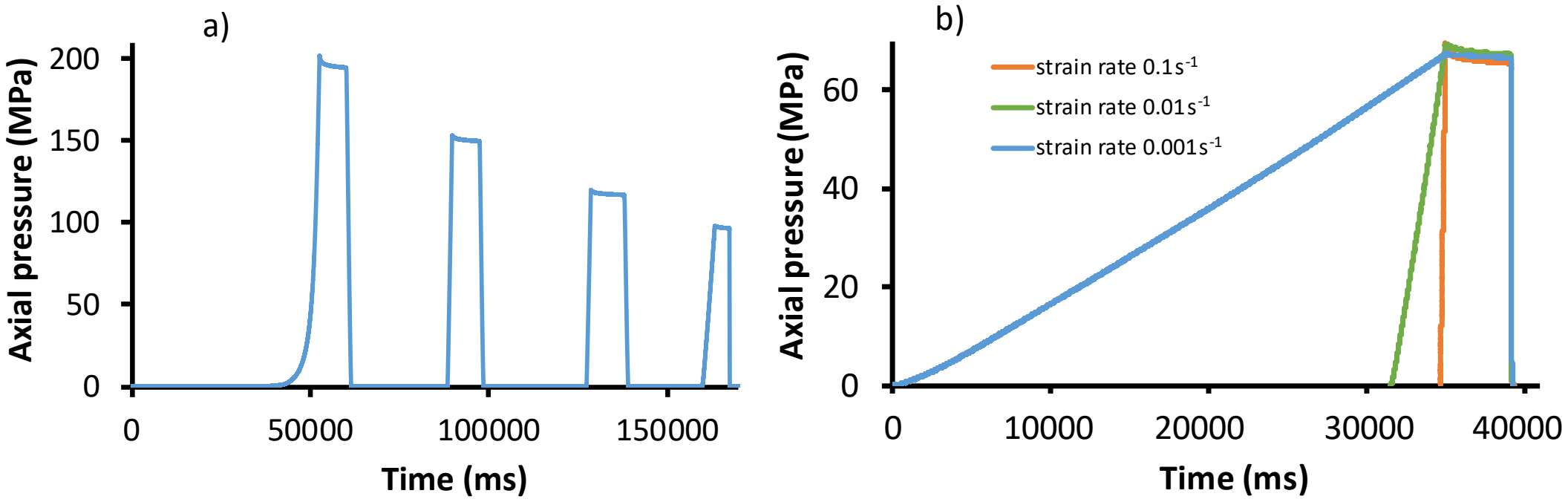
a)
Axial pressure (MPa)
200
150
100
50
0
0
50000
100000
150000
Time (ms)
b)
Axial pressure (MPa)
60
40
20
0
strain rate 0.1s-1
strain rate 0.01s-1
strain rate 0.001s-1
0
10000
20000
30000
40000
Time (ms)

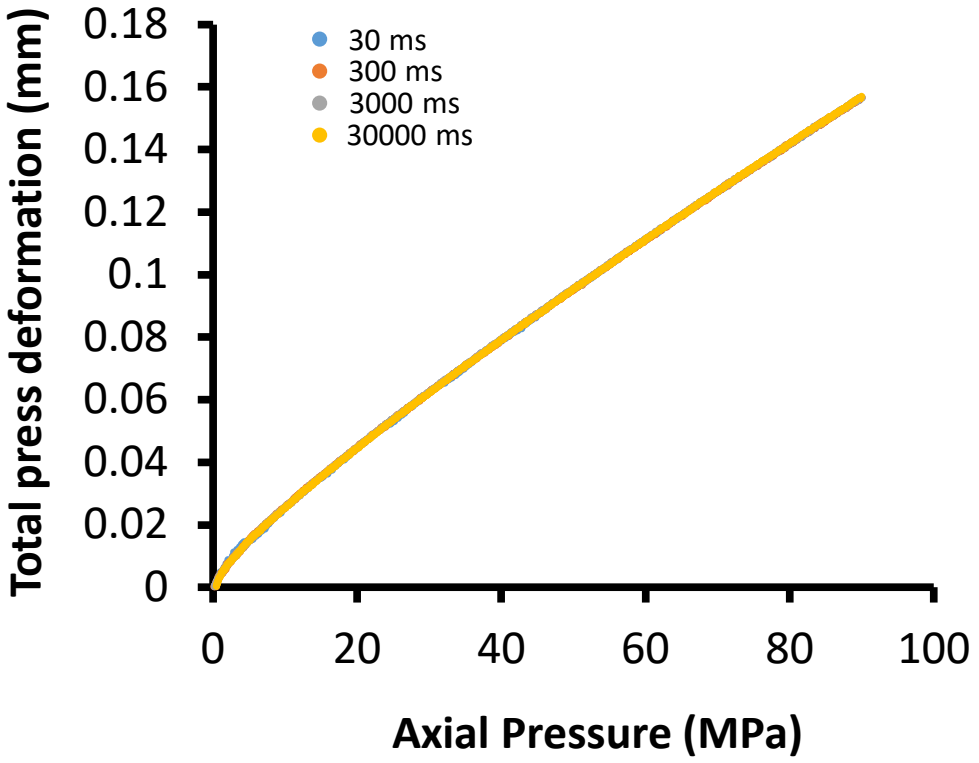
Total press deformation (mm)
0.18
0.16
0.14
0.12
0.1
0.08
0.06
0.04
0.02
0
30 ms
300 ms
3000 ms
30000 ms
0
20
40
60
80
100
Axial Pressure (MPa)

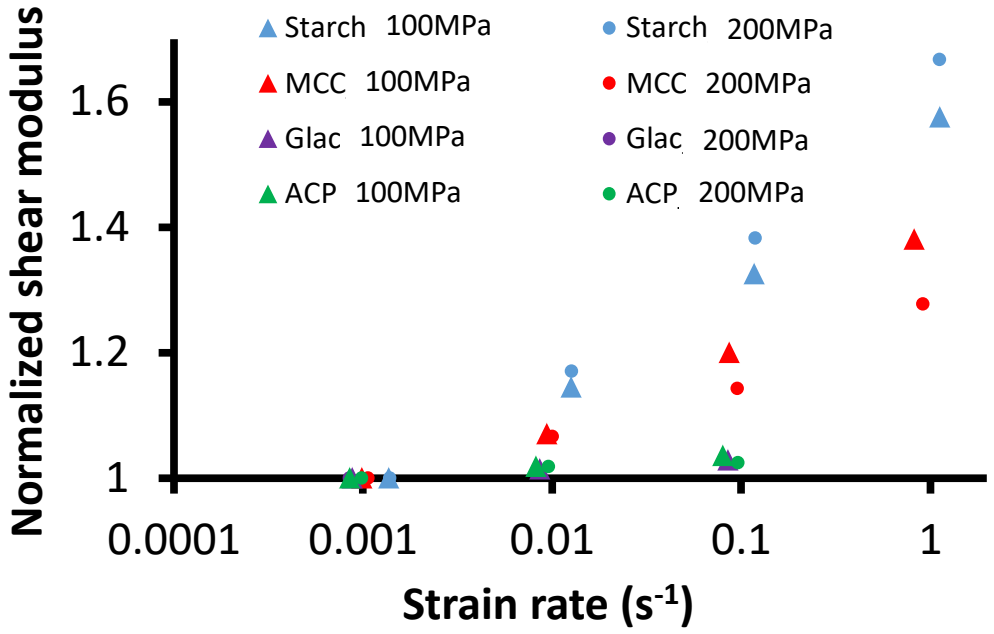
Normalized shear modulus
1.6
1.4
1.2
1
0.0001
0.001
0.01
0.1
1
Strain rate (s-1)
Starch 100MPa
MCC 100MPa
Glac 100MPa
ACP 100MPa
Starch 200MPa
MCC 200MPa
Glac 200MPa
ACP 200MPa

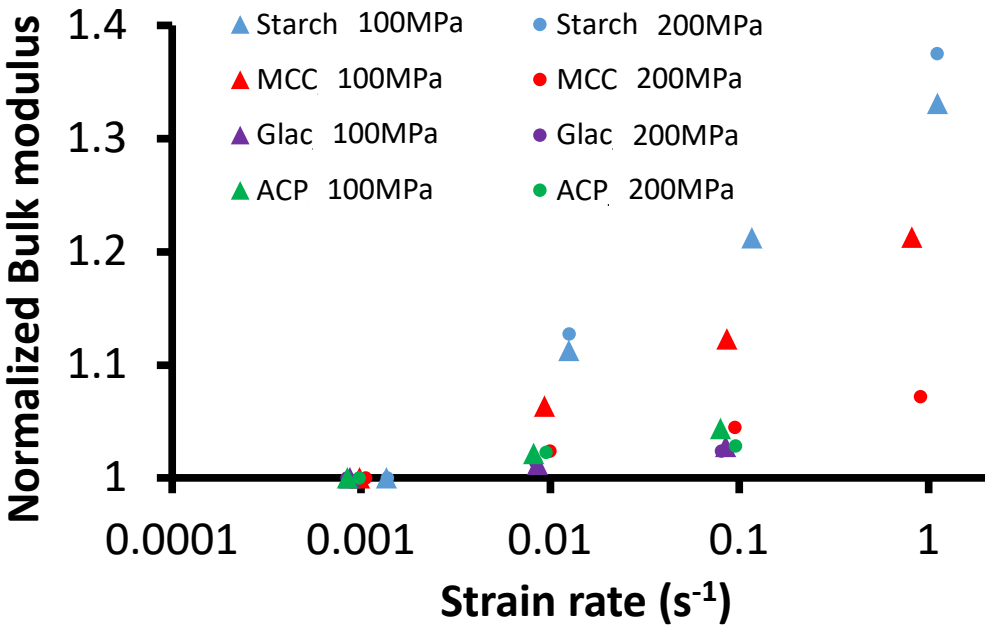
Normalized Bulk modulus
1.4
1.3
1.2
1.1
1
Starch 100MPa
MCC 100MPa
Glac 100MPa
ACP 100MPa
Starch 200MPa
MCC 200MPa
Glac 200MPa
ACP 200MPa
0.0001
0.001
0.01
0.1
1
Strain rate (s-1)

Table 1: Porosity of the tablets obtained after ejection. True density was determined using Helium pycnometry (Accupyc 1340, Micromeretics, Norcross, USA).

Product	True density ($g.cm^{-3}$)	First compression pressure (MPa)	Porosity(%)
ACP	2.857	100	32.4 ± 0.1
		200	26.2 ± 0.1
Glac	1.549	100	16.2 ± 0.1
		200	10.2 ± 0.1
MCC	1.566	100	12.3 ± 0.2
		200	5.9 ± 0.3
Starch	1.485	100	10.5 ± 0.3
		200	6.4 ± 0.1

Table 2: Apparent elastic constants obtained for all the products (standard deviation between parentheses)

Apparent elastic moduli		E (MPa)		ν		G(MPa)		K(MPa)	
First compression pressure (MPa)		100	200	100	200	100	200	100	200
Product	Loading time (ms)								
MCC	30000	1428 (19.4)	2005 (11.7)	0.323 (0.002)	0.357 (0.001)	540 (7.6)	739 (5.0)	1344 (18.5)	2331 (6.5)
	3000	1529 (19.1)	2130 (16.3)	0.322 (0.002)	0.351 (0.002)	578 (7.6)	788 (6.9)	1429 (16.6)	2386 (8.8)
	300	1700 (27.5)	2273 (25.5)	0.312 (0.002)	0.344 (0.002)	648 (11.2)	845 (10.5)	1508 (14.9)	2436 (4.5)
	30	1941 (27.3)	2517 (25.6)	0.301 (0.002)	0.332 (0.002)	746 (11.2)	945 (11.1)	1629 (15.8)	2498 (13.9)
Starch	30000	634 (2.8)	681 (3.6)	0.337 (0.001)	0.344 (0.001)	237 (1.1)	253 (1.5)	649 (3.1)	729 (1.5)
	3000	723 (4.2)	795 (2.1)	0.333 (0.001)	0.339 (0.001)	271 (1.7)	297 (0.9)	722 (3.3)	822 (0.8)
	300	832 (10.2)	931 (4.7)	0.324 (0.001)	0.329 (0.001)	314 (4.1)	350 (1.9)	787 (5.0)	906 (2.5)
	30	979 (6.3)	1111 (7.4)	0.311 (0.004)	0.315 (0.001)	373 (3.2)	423 (3.1)	864 (15.6)	1003 (5.1)
ACP	20000	7336 (51.1)	9755 (36.4)	0.191 (0.001)	0.195 (0.001)	3079 (22.3)	4082 (17.2)	3959 (24.4)	5330 (19.3)
	2000	7480 (9.0)	9947 (35.2)	0.192 (0.001)	0.196 (0.001)	3138 (4.8)	4159 (18.6)	4043 (10.7)	5450 (7.7)
	200	7613 (12.1)	10005 (76.1)	0.193 (0.001)	0.196 (0.001)	3191 (6.3)	4184 (34.2)	4131 (8.2)	5481 (32.9)
Glac	17000	4380 (42.3	5221 (24.2)	0.244 (0.001)	0.267 (0.001)	1760 (17.3)	2060 (10.2)	2857 (25.8)	3738 (14.5)
	1700	4441 (16.1)	5282 (10.7)	0.244 (0.001)	0.268 (0.001)	1785 (6.9)	2083 (5.0)	2890 (10.4)	3789 (11.7)
	170	4505 (13.2)	5374 (14.2)	0.244 (0.001)	0.266 (0.001)	1810 (6.2)	2123 (6.0)	2936 (6.1)	3827 (7.5)

Table 3: Comparison of the moduli G and K between the experiments and the analytical approach for MCC and Starch

Product	First compression pressure (MPa)	Strain rate (s^{-1})	G (MPa)		K (MPa)	
			Experiment	Analytic	Experiment	Analytic
MCC	100	1.000	746	747	1629	1632
		0.100	648	649	1508	1511
		0.010	578	580	1429	1431
		0.001	540	541	1344	1346
	200	1.000	945	946	2498	2502
		0.100	845	847	2436	2440
		0.010	788	790	2386	2390
		0.001	739	741	2331	2335
Starch	100	1.000	373	374	864	865
		0.100	314	315	787	788
		0.010	271	272	722	724
		0.001	237	237	649	650
	200	1.000	423	423	1003	1005
		0.100	350	351	906	907
		0.010	297	297	823	824
		0.001	253	254	730	731

Table 4: Parameters of the Prony series for MCC and Starch

Product	**First comp load (MPa)**	**G_i**	**K_i**	**T_i**	**E_∞(MPa)**	**ν_∞**
MCC	100	0.2330	0.1345	30	1400.8	0.323
		0.1390	0.0290	300		
		0.1130	0.1090	3000		
	200	0.1990	0.0377	30	1978.7	0.358
		0.0540	0.0107	300		
		0.1120	0.0405	3000		
Starch	100	0.3410	0.1685	30	619.7	0.338
		0.1490	0.0480	300		
		0.2430	0.1950	3000		
	200	0.3860	0.1880	30	664.7	0.346
		0.1780	0.0590	300		
		0.2880	0.2200	3000		

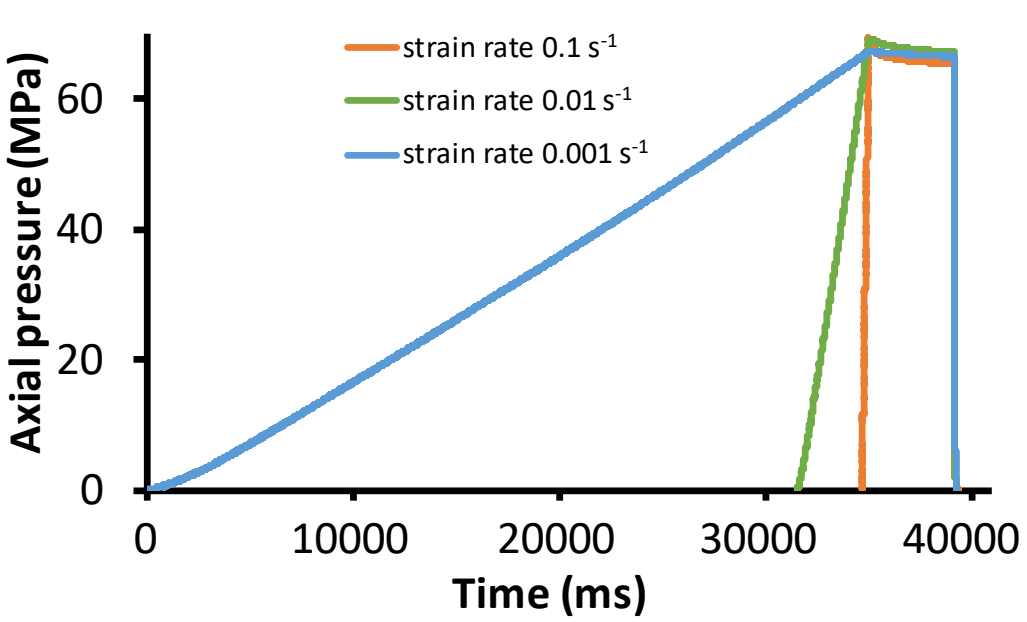
strain rate 0.1 s-1
strain rate 0.01 s-1
strain rate 0.001 s-1
Axial pressure (MPa)
0
20
40
60
0
10000
20000
30000
40000
Time (ms)

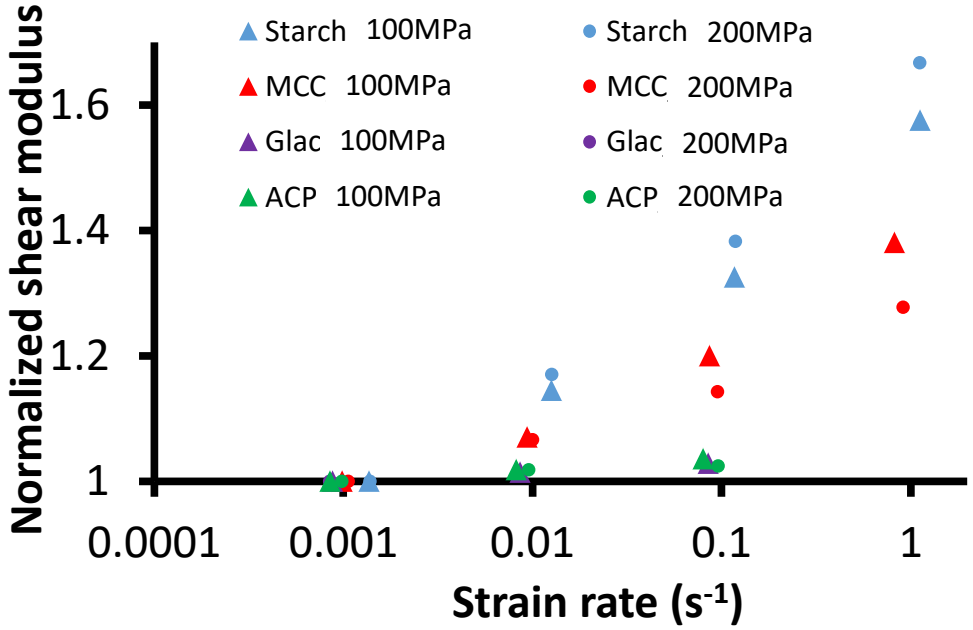
Starch 100MPa
MCC 100MPa
Glac 100MPa
ACP 100MPa
Starch 200MPa
MCC 200MPa
Glac 200MPa
ACP 200MPa
Normalized shear modulus
1
1.2
1.4
1.6
0.0001
0.001
0.01
0.1
1
Strain rate (s-1)